Journal of Power Sources 195 (2010) 3407–3415

Contents lists available at ScienceDirect

Journal of Power Sources

journal homepage: www.elsevier.com/locate/jpowsour

Direct methanol fuel cell based on poly(vinyl alcohol)/titanium oxide nanotubes/poly(styrene sulfonic acid) (PVA/nt-TiO_2/PSSA) composite polymer membrane

Chun-Chen Yang*, Wen-Chen Chien, Yingjeng James Li

Department of Chemical Engineering, Ming Chi University of Technology, 84 Gungjuan Rd., Taishan, Taipei Hsien 243, Taiwan, ROC

ARTICLE INFO

Article history:
Received 6 November 2009
Received in revised form 5 December 2009
Accepted 7 December 2009
Available online 14 December 2009

Keywords:
Poly(vinyl alcohol) (PVA)
Nanotube-titanium oxide (nt-TiO_2)
Poly(styrene sulfonic acid) (PSSA)
Proton-conducting composite membrane
Direct methanol fuel cell (DMFC)

ABSTRACT

The high performance poly(vinyl alcohol)/titanium oxide nanotubes/poly(styrene sulfonic acid) (PVA/nt-TiO_2/PSSA) proton-conducting composite membrane is prepared by a solution casting method. The characteristic properties of these blend composite membranes are investigated by thermal gravimetric analysis (TGA), scanning electron microscopy/energy dispersive X-ray spectroscopy (SEM/EDX), micro-Raman spectroscopy, dynamic mechanical analysis (DMA), methanol permeability measurement and AC impedance method. It is found that the peak power densities of the DMFC with 1, 2, and 4 M CH_3OH fuels are 12.85, 23.72, and 10.99 mW cm^{-2}, respectively, at room temperature and ambient air. Especially, among three methanol concentrations, the 2 M methanol shows the highest peak power density among three methanol concentrations. The results indicate that the air-breathing direct methanol fuel cell comprised of a novel PVA/nt-TiO_2/PSSA composite polymer membrane has excellent electrochemical performance and stands out as a viable candidate for applications in DMFC.

1. Introduction

Methanol is often used as a fuel for direct methanol fuel cells (DMFCs). DMFCs are recently gaining much attention for their highly potential in applications such as electric vehicles (EVs), stationary applications, and portable power sources, such as cellular phones, notebook computers, etc. At the present time, DMFCs are being actively studied and have gained a lot of progress during the past few years [1–17]. However, the development of the DMFC has been hampered due to several serious problems, which are the slow methanol oxidation kinetics and incomplete electrooxidation of methanol, the poisoning of adsorbed intermediate species on the Pt surface, the high methanol crossover through Nafion polymer membrane, and the high costs of Nafion polymer membrane and Pt catalyst.

Nowadays, the perfluorosulfonate ionomer membranes, such as Nafion membranes (Du Pont), are the primary polymer membranes used on the DMFCs. However, the commercial Nafion polymer membrane showed a serious methanol crossover problem, in which methanol permeates from the anode to the cathode. The methanol permeation not only causes a loss of fuel but also forms a mixed potential at the cathode and leads to a lower electrochemical performance. Thus, for the liquid methanol fuel cell, it is imperative that a solid polymer membrane used in a DMFC have a lower methanol permeability rate, i.e., be absent of methanol crossover problem.

As examples, Yang et al. [18,19] synthesized the cross-linked PVA/MMT composite polymer membrane and demonstrated it for acidic DMFCs. However, a challenge for PVA-based polymer membranes is that they show a poor proton conductivity and the acidic electrolyte may leak out from the PVA polymer membranes. The main reason for this problem is that PVA polymer itself does not contain any negatively charged ions or the negative organic functional groups, like carboxylic (–COOH) or sulfonic acid (–SO_3H). If we want to PVA polymer membrane could be used in the DMFC, some negatively charged ions needed to be grafted or blended into PVA polymer host. From this point of view, we choose the poly(styrene sulfonic acid) (PSSA) as a donor, which would be expected to give the reasonable proton conductivity for the PVA/PSSA blend composite polymer membrane. Rhim et al. [20] prepared the PVA/sulfosuccinic acid (SSA) proton-conducting polymer membrane; the SSA containing –SO_3H and –COOH groups was used as a cross-linking agent and also as a proton donor, which varied in the range 5–30 wt.%.

Recently, some authors [21,22] prepared the double-layer membranes based on sulfonated poly(ether ether ketone)/poly(vinyl alcohol) (SPEEK/PVA blend) for a DMFC. The sub-layer rich in PVA clung to the anode and provided a good barrier for the methanol crossover. The SPEEK sub-layer was used to maintain the mechanical stability and low swelling ratio. Inter-

* Corresponding author. Tel.: +886 29089899; fax: +886 29041914.
E-mail address: ccyang@mail.mcut.edu.tw (C.-C. Yang).

0378-7753/$ – see front matter © 2009 Elsevier B.V. All rights reserved.
doi:10.1016/j.jpowsour.2009.12.024

estingly, Kumar et al. [23] studied the poly(vinyl alcohol)/para toluene sulfonic acid (PVA/PTSA) polymer membranes for a DMFC. By introducing a suitable amount of proton charge carriers (namely, $-SO_3H$ group), the ionic conductivity of PVA/PTSA polymer membrane was enhanced by this hydrophilic PTSA. The membrane prepared with 10 wt.%PVA/10 wt.%PTSA exhibited a high selectivity in the range of 12.7×10^7 mS s cm^{-3}, which is more than three times grater than that of Nafion 117 membrane. Moreover, Sahu et al. [24] investigated the effect of poly(styrene sulfonic acid) content on the PVA–PSSA blend polymer membrane and its application for a hydrogen–oxygen polymer electrolyte membrane fuel cell (PEMFC). They found that a maximum proton conductivity of PVA/PSSA blend polymer membrane was observed with 35 wt.%PSSA. A peak power density of 210 mW cm^{-2} at 500 mA cm^{-2} was achieved for the PEMFC with the optimized PVA/PSSA polymer membrane at 75 °C, as compared to a peak power density of only 38 mW cm^{-2} observed at 80 mA cm^{-2} for the PEMFC with the pristine PVA membrane.

Poly(styrene sulfonic acid) polymer was here used as a proton source in this work, the fixed amount of 20 wt.%PSSA (i.e., PVA:PSSA = 1:0.20) was blended into the PVA host. In addition, titanium oxide (TiO_2, also called titania) has been extensively studied owing to its outstanding physical and chemical properties. Titania is typically used in the form of nano-particles providing high surface area and activity, and excellent chemical stability. The addition of these hydrophilic nano-sized titanium oxide (TiO_2) fillers into the polymer matrix reduces the crystallinity of the PVA polymer, therefore increasing the amorphous phases of PVA polymer matrix, resulting in an increase of its ionic conductivity [19]. There are various types of ceramic fillers; for examples TiO_2 (PVA/TiO_2) [25], SiO_2 (PEG/SiO_2 and PVA/SiO_2) [26], hydroxyapatite (PVA/HAP) [27], have been used. As have been demonstrated, when these nanotube TiO_2 fillers, with high specific surface area, are used as stiffener materials by being added to the polymer matrix, the methanol permeability of the composite polymer membrane can be effectively reduced [18].

In this work, we attempted to disperse nt-TiO_2 fillers into the PVA and PSSA polymer matrix as the solid plasticizers, which were capable of enhancing the chemical and thermal properties, and dimensional stability for the PVA/nt-TiO_2/PSSA composite membrane. TGA was used to analyze the thermal stability properties of the PVA/nt-TiO_2/PSSA proton-conducting composite membrane. DMA was applied to study the mechanical properties of the composite polymer membranes. SEM/EDX was employed to examine the surface morphology and the composition of the composite polymer membranes. Micro-Raman spectroscopy was used to investigate the chemical properties of PVA/nt-TiO_2/PSSA composite membranes. A diffusion cell was designed to measure the methanol permeability of PVA/nt-TiO_2/PSSA composite membranes. The ionic conductivity of PVA/nt-TiO_2/PSSA composite polymer electrolytes was measured by AC impedance spectroscopy. The characteristic properties of PVA/nt-TiO_2/PSSA composite membranes with different amounts (1.5–10 wt.%) of nt-TiO_2 fillers (as the functions of a solid plasticizer as well as a methanol permeability barrier) and 20 wt.%PSSA polymer (as a proton donor) were examined and discussed in detail.

Finally, the DMFC, composed of the air cathode, the anode, and the PVA/nt-TiO_2/PSSA composite polymer membrane, was assembled and investigated. For comparison, the methanol concentration was varied in the range of 1–4 M. The electrochemical characteristics of the DMFC employing PVA/nt-TiO_2/PSSA composite membranes were investigated by the linear polarization, potentiostatic and galvanostatic methods; especially for the peak power density of the DMFC.

2. Experimental

2.1. Preparation of the PVA/nt-TiO_2/PSSA composite membrane

PVA (Aldrich), PSSA (Aldrich, 18 wt.% solution), nano-sized TiO_2 fillers (50 nm, 50 m^2 g^{-1}, P25, Degussa) and H_2SO_4 (Merck) were used as received without further purification. The nt-TiO_2 powders (used P25 TiO_2 as a raw material) were prepared by a hydrothermal method (autoclave) at 130–150 °C for 12 h in a 10 M NaOH solution under a continuous stirring condition [28]. The pH of the as-prepared TiO_2 powders solution was adjusted to 5 to form nanotube TiO_2, and then washed with D.I. water several times, filtered and dried for further use. Degree of polymerization and saponification of PVA were 1700 and 98–99%, respectively. The PVA/nt-TiO_2/PSSA composite membrane was prepared by a solution casting method. The varied weight percents (1.5–10 wt.%) of nt-TiO_2 fillers were added slowly in distilled water under a constant stirring condition.

The above resulting solution was stirred continuously at 85 °C for 2 h until becoming homogeneous and viscous. The contents of nt-TiO_2 fillers in the PVA and PSSA matrix were well controlled. About 5 wt.% glutaraldehyde (GA, 50 wt.% content in distilled water, Merck) was finally added into the viscous mixture polymer solution to carry out the cross-linking reaction. The resulting viscous blend polymer solution was coated onto a glass plate.

The thickness of the wet composite polymer membrane is between 0.20 and 0.40 mm. The glass plate with viscous PVA/nt-TiO_2/PSSA composite polymer sample was weighed again and then the excess water was allowed to evaporate slowly at 60 °C with a relative humidity of 30%. After evaporation of the water solvent, the glass plate with the composite polymer membrane was weighed again. The composition of PVA/nt-TiO_2/PSSA composite polymer membrane was determined from the mass balance. The thickness of the dried composite polymer membrane was controlled in the range of between 0.10 and 0.20 mm. The preparation methods of the composite polymer membranes based on PVA by a solution casting method have been reported in detail [18,19].

2.2. Surface morphology, thermal and mechanical properties

The surface morphology and composition of all PVA/nt-TiO_2/PSSA composite membranes were investigated using a Hitachi S-2600H scanning electron microscope with energy dispersive X-ray spectroscopy (SEM/EDX). TGA thermal analysis was carried out using a Mettler Toledo TGA/SDT 851 system. Measurements were carried out by heating from 25 to 600 °C under N_2 atmosphere at a heating rate of 10 °C min^{-1} with about 10 mg sample. Dynamic mechanical analyses (DMA) were conducted using a RSA-III Instrument DMA-Thermal analyzer (TA) at a frequency of 1 Hz and oscillation amplitude of 0.15 mm. DMA measurements were carried out by heating from 25 to 150 °C under an air atmosphere at a heating rate of 5 °C min^{-1}.

2.3. Ionic conductivity and methanol permeability measurements

Conductivity measurements were made for PVA/nt-TiO_2/PSSA composite membranes via AC impedance method. The PVA/nt-TiO_2/PSSA composite were first immersed in a 2 M H_2SO_4 solution for at least 24 h, and then washed with D.I. water three times before test. These composite membranes were clamped between stainless steel (SS304), ion-blocking electrodes, each of surface area 1.32 cm^2, in a spring-loaded glass holder. A thermocouple was kept in close proximately to the composite polymer membrane for temperature measurement. Each sample was equilibrated at the experimental temperature for at least 60 min before measurement. AC impedance measurements were carried out using

an Autolab PGSTAT-30 equipment (Eco Chemie B.V., Netherlands). The AC spectra in the range of 100 kHz to 10 Hz at an excitation signal of 5 mV were recorded. AC impedance spectra of the composite polymer membrane were recorded at a temperature range between 30 and 70 °C. Experimental temperatures were maintained within ±0.5 °C by a convection oven. All PVA/nt-TiO_2/PSSA composite membranes were examined at least three times.

Methanol permeability measurements were conducted utilizing a diffusion cell [18]. The cell was divided into two compartments, in which one compartment was filled with D.I. water (called B compartment) and the other compartment filled with a 20 wt.% methanol aqueous solution (called A compartment). Prior to testing, the PVA/nt-TiO_2/PSSA composite membrane was hydrated in D.I. water for at least 24 h. The composite polymer membrane with a surface area of 0.58 cm^2 was sandwiched by O-ring and clamped tightly between the two compartments. A stir bar was kept active in the glass diffusion cell during the experiment. The concentration of methanol diffused from compartment A to B across the PVA/nt-TiO_2/PSSA composite membrane was examined vs. time using a density meter (Mettler Toledo, DE45). An aliquot of 0.20 mL was sampled from the B compartment every 30 min. Before the permeation experiment, the calibration curve for the value of density vs. the methanol concentration was prepared. The calibration curve was used to calculate the methanol concentration in the permeation experiment. The methanol permeability was calculated from the slope of the straight-line plot of the methanol concentration vs. the permeation time. The methanol concentration in the B compartment as a function of time is given in Eq. (1):

$$C_B(t) = \frac{A}{V}\frac{DK}{L}C_A(t - t_o) \quad (1)$$

where C_A is the methanol concentration, A and L are the proton-conducting composite polymer membrane area and thickness; D and K are the methanol diffusivity and partition coefficient between the membrane and the solution. The product DK is the membrane permeability (P), t_o, also termed time lag, is related to the diffusivity: $t_o = L^2/6D$.

2.4. Micro-Raman spectroscopy analyses

Micro-Raman spectroscopy is a powerful tool to characterize the PVA/nt-TiO_2/PSSA composite membrane. The micro-Raman spectroscopy analysis was carried out using a Renishaw confocal microscopy Raman spectroscopy system with a microscope equipped with a 50× objective and a charge coupled device (CCD) detector. Raman excitation source was provided by a 632.8 nm He–Ne laser beam, which had a beam power of 17 mW and was focused on the sample with a spot size of about 1 μm in diameter.

2.5. Preparation of the anode and the cathode

The catalyst slurry ink of the anode was prepared by using PtRu black (Alfa, HiSPEC 6000, PtRu black with Pt:Ru = 1:1 molar ratio), 15 wt.% Nafion binder solution (Aldrich), and a suitable amount of distilled water and IPA. The resulting PtRu black inks were first ultrasonicated for 2 h. The PtRu black inks were loaded onto the carbon paper (GDL 10BB, SIGRACET, Germany) by a paint-brush method to achieve a loading of 4 mg cm^{-2}. The as-prepared anode was dried in a vacuum oven at 110 °C for 2 h. Similarly, the air cathode was prepared using the same procedure as the anode but the cathode with a Pt black catalyst of 4.0 mg cm^{-2}.

2.6. Electrochemical measurements

The PVA/nt-TiO_2/PSSA composite membrane was sandwiched between the sheets of the anode and cathode and then hot-pressed at 25 °C under 100 kg_f cm^{-2} for 15 min to obtain a membrane electrode assembly (MEA). The electrode area of the MEA was about 1 cm^2.

The electrochemical measurements were also carried out in a two-electrode system. The *I–t*, *E–t*, *I–V* and the power density (P.D.) curves for the DMFC comprised of the PVA/nt-TiO_2/PSSA composite membrane were recorded for various cell potentials and current densities at a scan rate of 1 mV s^{-1}, respectively. All electrochemical measurements were performed on an Autolab PGSTAT-30 electrochemical system with GPES 4.8 package software (Eco Chemie, Netherlands). The electrochemical performances of the DMFC, employing a PVA/nt-TiO_2/PSSA proton-conducting composite membrane, were systematically examined with 1–4 M methanol fuels, respectively, at an ambient temperature, as shown in Fig. 1.

3. Results and discussion

3.1. Thermal analyses

Fig. 1(a) shows TGA thermographs for pure PVA, PVA/20 wt.%PSSA (without nt-TiO_2) and PVA/1.5–10 wt.%nt-TiO_2/20 wt.%PSSA composite membranes, respectively. The TGA curve of the PVA/*X*%nt-TiO_2/20 wt.%PSSA polymer membranes shows four major weight loss regions, which appear as four major peaks in the DTG curves, as shown in Fig. 1(b). The first region at a temperature of 80–100 °C ($T_{p,1}$ = 100 °C) is due to the evaporation of weakly physical and strongly chemical bound H_2O; the weight loss of the membrane is about 2–3 wt.%. The second transition region at around 176–182 °C ($T_{p,2}$ = 180 °C) is due to the degradation of the PVA/nt-TiO_2/PSSA composite membrane, the total weight loss corresponds to this phase, about 27–31 wt.%. The peak of the third transition at around 300–322 °C ($T_{p,3}$ = 319 °C) is due to the cleavage of the side-chain of PSSA polymer (or called desulfonation), the total weight loss is about 34–38 wt.% at 300 °C. The fourth transition region at around 410–460 °C ($T_{p,4}$ = 439 °C) is due to the cleavage of the backbone of PVA polymer membrane, reflecting a the total weight loss of about 72–78 wt.% at 600 °C.

Accordingly, the degradation peaks of cross-linked PVA/nt-TiO_2/PSSA proton-conducting composite polymer samples are less intense and shift towards higher temperature. It can be concluded that the thermal stability is improved probably due to the additive effect of nt-TiO_2 fillers and the chemical cross-linked reaction between the PVA and glutaraldehyde.

3.2. Surface morphology

SEM photographs of top and cross-sections views of the PVA/10 wt.%nt-TiO_2/20 wt.%PSSA composite polymer membrane are shown in Fig. 2(a) and (b), at a magnification of 2000× and 1000×, respectively. It was revealed that some nt-TiO_2 aggregates or chunk were formed within the PVA/nt-TiO_2/PSSA composite membranes. The dimension of these nt-TiO_2 aggregates embedded in the PVA matrix was around 0.2–2 μm; the surface morphology of as-prepared nt-TiO_2 fillers is shown in the inset of Fig. 3(b). Note that these nt-TiO_2 fillers were made by a hydrothermal process at 130 °C for 12 h in a 10 M NaOH solution under a continuous stirring condition. The specific surface area (around 197.3 m^2 g^{-1}) for nt-TiO_2 fillers was much higher than that of P25 TiO_2 powders (only 51.8 m^2 g^{-1}). Apparently, as SEM results indicated that the higher content of nt-TiO_2 fillers tended to cause formation of aggregates and thus caused a poor dispersion in the PVA/PSSA blend polymer; particularly when the content of nt-TiO_2 fillers was over 10 wt.%.

In general, both hydrophilic PVA polymer and nt-TiO_2 fillers were homogeneous and fully compatible without any phase separation occurring while the suitable amount of nt-TiO_2 ceramic

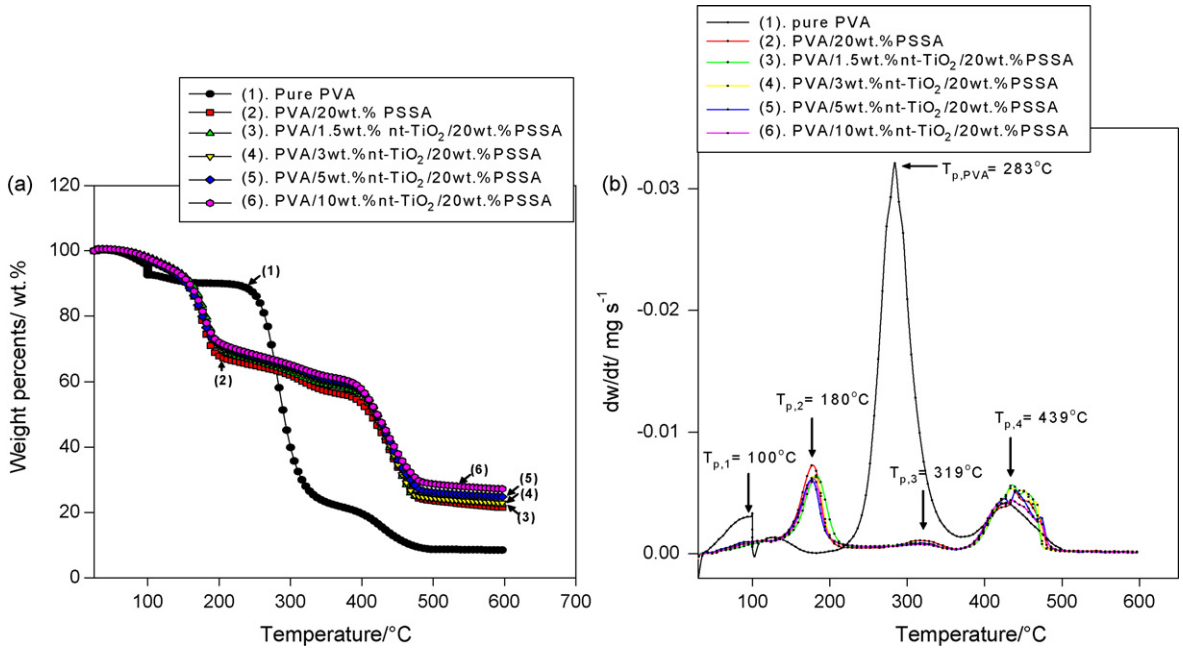

Fig. 1. (a) TGA and (b) DTG thermographs for pure PVA film, PVA/20 wt.%PSSA, and PVA/1.5–10 wt.%nt-TiO_2/20 wt.%PSSA composite polymer membranes.

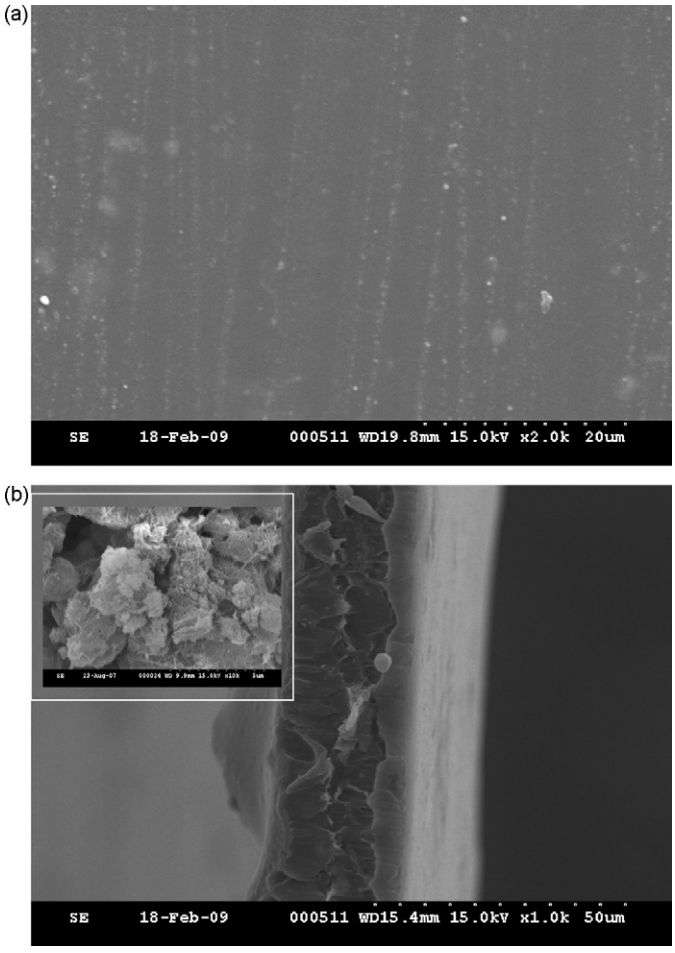

Fig. 2. SEM photographs for a PVA/10 wt.%nt-TiO_2/20 wt.%PSSA composite polymer membrane: (a) top-view, (b) cross view, the inset for nt-TiO_2 fillers.

fillers was added. It is well accepted that the suitable amount of nt-TiO_2 fillers (as the methanol diffusion barriers) can greatly increase the tortuosity path for the methanol diffusion, which reduce the methanol crossover rate for the composite polymer membranes [18,27]. Thus, the addition of nt-TiO_2 fillers in the PVA/PSSA blend polymer membrane can markedly reduce methanol crossover rate.

3.3. Micro-Raman analysis and mechanical properties

Fig. 3(a) shows the micro-Raman spectra of pure PVA, pure PSSA and PVA/3 wt.%nt-TiO_2/20 wt.%PSSA composite membranes. The spectra showed some strong characteristic scattering peaks for PVA polymer at 1440, 1258, 1146, 919, and 860 cm^{-1}. For PSSA, strong characteristic scattering peaks for PSSA polymer were at 1598, 1192, 1125, and 1038 cm^{-1}. Fig. 3(b) shows the micro-Raman spectra of pure PVA, the PVA/20 wt.%PSSA and PVA/1.5–10 wt.%nt-TiO_2/20 wt.%PSSA composite membranes. Several strong characteristic scattering peaks of nt-TiO_2 fillers at 145, 398, 517 and 638 cm^{-1} were identified for O–Ti–O; they were due to the Ti–O bending and stretching vibrations (not shown here). A very strong peak for the PVA polymer at 1440 cm^{-1} was due to the C–H bending and O–H bending. In addition, two additional vibrational peaks for PVA polymer at 919 and 860 cm^{-1} were due to the C–C stretching. There were several weak scattering peaks at 1258, 1146, 1093, and 1066 cm^{-1}; they were due to the C–C stretching and C–O stretching, as also shown in Fig. 3(a). Three strong scattering peaks for PSSA polymer at 1598, 1192, and 1125 cm^{-1} were found. More specifically, the peaks of 1598 and 1192 cm^{-1} were due to the C=C stretching and the peak of 1125 cm^{-1} was due to the $-SO_3^-$ stretching, as shown in Fig. 3(b)

The most important outcome with respect to the micro-Raman analysis, it can be clearly seen that the intensities of these characteristic vibrational peaks for PVA/nt-TiO_2/PSSA composite membranes are slightly varied; a vibrational peak of the $-SO_3^-$ at 1126 cm^{-1} is an indicator for PSSA polymer [23]. In other words, it indicated that the ionic groups ($-SO_3^-$) indeed existed in the PVA/nt-TiO_2/PSSA composite membrane. The addition of PSSA polymer containing the sulfonic group blend into the PVA matrix will greatly enhance the proton conductivity and it also can prevent proton charge carriers from being lost from the composite polymer electrolyte [20].

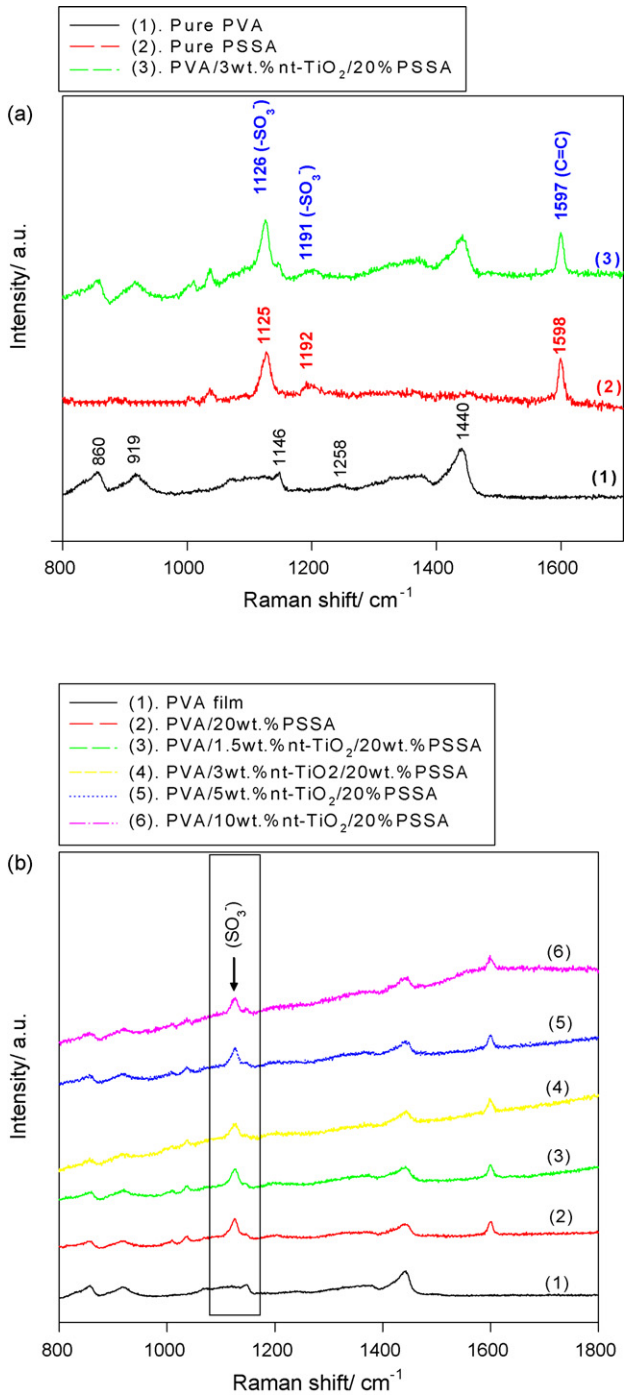

Fig. 3. Micro-Raman spectra: (a) PVA film, PSSA film, and PVA/3 wt.%nt-TiO_2/20 wt.%PSSA composite polymer membrane, (b) PVA/*X* wt.%nt-TiO_2/20 wt.%PSSA polymer membranes.

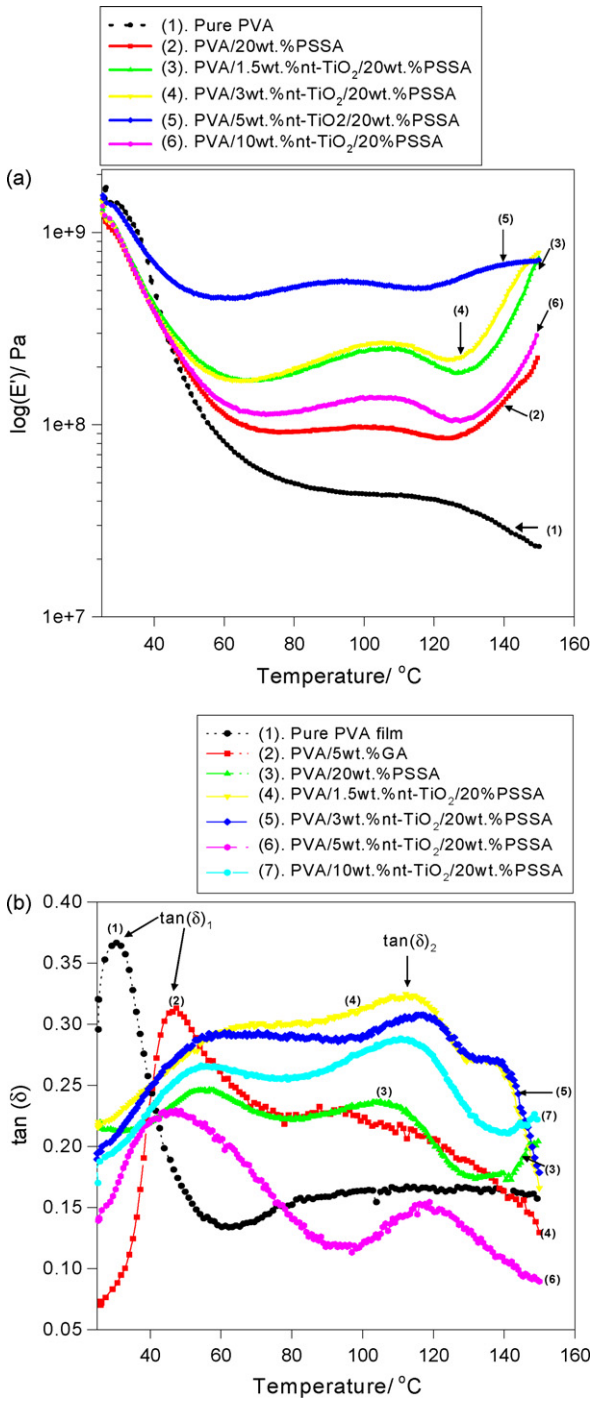

Fig. 4. DMA spectra for PVA/*X* wt.%nt-TiO_2/20 wt.%PSSA composite polymer membranes: (a) E'' vs. T and (b) tan(δ) vs. T.

Fig. 4(a) shows the variation of storage modulus (E') vs. temperature for pure PVA, PVA/20 wt.%PSSA and PVA/1.5–10 wt.%nt-TiO_2/20 wt.%PSSA composite membranes. The storage modulus of pure PVA ($E' = 1.35 \times 10^9$ Pa) was higher than these of PVA/nt-TiO_2/20 wt.%PSSA composite membranes ($E' = 9.03 \times 10^8$ to 1.21×10^9 Pa) at 30 °C. It was found that the storage modulus of PVA/nt-TiO_2/PSSA composite membranes was increased with increasing nt-TiO_2 fillers loading (up to 5 wt.%). The storage modulus had decreased when the content of nt-TiO_2 fillers was 10 wt.%, as listed in Table 1. It may be due to the poor dispersion of nt-TiO_2 fillers in the composite polymer membrane; it indirectly results in

Table 1
The storage modulus (E') values for PVA/*X* wt.%nt-TiO_2/20 wt.%PSSA composite polymer membranes at various temperatures.

Contents of nt-TiO_2	E'/Pa			
	30 °C	60 °C	100 °C	150 °C
Pure PVA film	1.35×10^9	7.84×10^7	4.35×10^7	2.32×10^7
0 wt.%	9.03×10^8	1.17×10^8	9.74×10^7	2.23×10^8
1.5 wt.%	9.30×10^8	1.78×10^9	2.41×10^8	1.35×10^8
3 wt.%	1.00×10^9	1.75×10^8	2.60×10^8	7.91×10^8
5 wt.%	1.21×10^9	4.58×10^8	5.50×10^8	7.18×10^8
10 wt.%	9.62×10^8	1.30×10^8	1.38×10^8	2.92×10^8

Table 2
The tan(δ) values for PVA/X wt.%nt-TiO_2/20 wt.%PSSA composite polymer membranes at various temperatures.

Contents of nt-TiO_2	T/°C	
	Tan(δ)$_1$[a]	Tan(δ)$_2$
Pure PVA film	30.38	–
0 wt.%	55.45	–
1.5 wt.%	65.62	112.89
3 wt.%	56.63	116.50
5 wt.%	47.29	117.61
10 wt.%	55.61	111.44

[a] The tan(δ)$_1$ value taken as a glass transition temperature of the PVA polymer ($T_{g,PVA}$).

poor physicochemical properties of the composite polymer membranes.

As a matter fact, the poor physicochemical properties (mechanical properties and methanol crossover rate) of the PVA/nt-TiO_2/PSSA composite membrane were found when the content of nt-TiO_2 fillers was over 10 wt.%. Thus, the amount of nt-TiO_2 fillers in the PVA/nt-TiO_2/PSSA composite membrane needs to be well controlled.

In summary, the optimal content of nt-TiO_2 fillers in the PVA/nt-TiO_2/PSSA composite membrane was 5 wt.%, which has a lower methanol permeability and reasonable ionic conductivity. Interestingly, it was also found that the mechanical properties were markedly improved when the thermal treatment was carried out at 120 °C. This may be due to the annealing effect on the cross-linked PVA-based composite membrane. In general, the annealing treatment will enhance the degree of cross-linking between the –OH group of the PVA polymer and the –CHO group of GA.

Fig. 4(b) shows the loss factor or tan(δ) vs. temperature curves of the PVA/nt-TiO_2/PSSA composite membranes. The glass transition temperatures (T_g) can be taken at a peak (tan(δ)$_1$) of the tan(δ) curve. The glass transition temperatures of pure PVA film ($T_{g,PVA}$) and all PVA/X%nt-TiO_2/20 wt.%PSSA composite membranes are listed in Table 2. The results indicated that the glass transition temperatures of pure PVA film (considered as a $T_{g,PVA}$) and the PVA/20 wt.%PSSA membrane were at 30.38 and 55.45 °C, respectively. Apparently, it was observed that there were two tan(δ) peaks, i.e., tan(δ)$_1$ and tan(δ)$_2$, for all PVA/X%nt-TiO_2/20 wt.%PSSA composite membranes. The tan(δ)$_1$ peak, it was taken as a $T_{g,PVA}$, which was located at between 47 and 65 °C; however, the tan(δ)$_2$ peaks were varied at between 111 and 118 °C. Interestingly, the tan(δ)$_2$ peaks were much broader for all PVA/X%nt-TiO_2/20 wt.%PSSA composite membranes.

The broader and lowering intensity for tan(δ)$_2$ peaks of PVA/X%nt-TiO_2/20 wt.%PSSA composite membranes may be due to the decrease of the degree crystallinity of the blend polymer membranes. The tan(δ)$_2$ peak temperature was appeared at around 100–120 °C when the nt-TiO_2 filler was added into the PVA/PSSA blend polymer membrane. It may be due to the slip of PVA polymer and PSSA polymer chains or the decreasing crystallinity of the PVA/nt-TiO_2/PSSA composite polymer membranes [18].

3.4. Ionic conductivity and methanol permeability

The typical AC impedance spectra of the PVA/nt-TiO_2/PSSA composite membrane, synthesized by blending PVA and PSSA (20 wt.%) polymers with 10 wt.%nt-TiO_2 fillers at different temperatures are shown in Fig. 5(a). The AC spectra are typically non-vertical spikes for stainless steel (SS) blocking electrodes, i.e., a SS|PVA/nt-TiO_2/PSSA SPE|SS cell. Analysis of the spectra yields information about the properties of the PVA/nt-TiO_2/PSSA composite membrane, such as bulk resistance, R_b. The bulk resistance associated the membrane conductivity was determined from the high-frequency

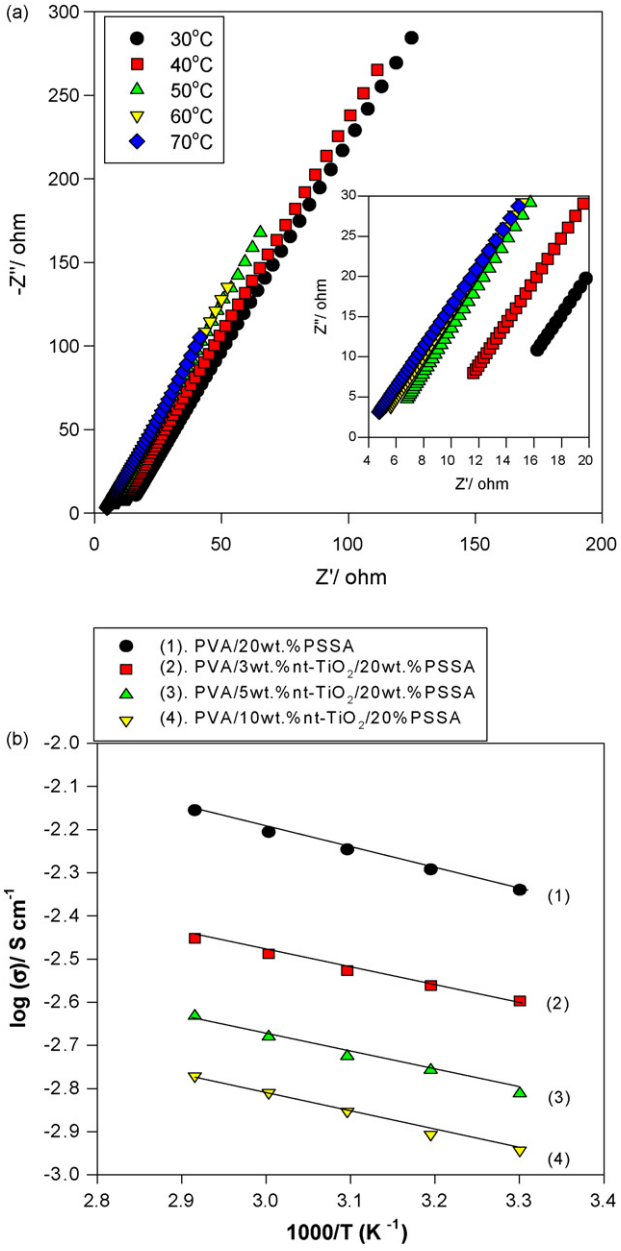

Fig. 5. (a) Nyquist plot for PVA/10 wt.%nt-TiO_2/20%PSSA composite polymer electrolytes in water at different temperatures; the inset for high-frequency range and (b) Arrhenius plot for PVA/X wt.%nt-TiO_2/20%PSSA composite membranes in water.

intercept of the impedance with real axis. Taking into account the thickness of the composite polymer membranes, the ionic conductivity (σ) was calculated from the R_b value, according to the equation: $\sigma = L/R_b \cdot A$, where σ is the proton conductivity of the composite membrane (S cm^{-1}), L is the thickness (cm) of the PVA/nt-TiO_2/PSSA composite membrane, A is the cross-sectional area of the blocking electrode (cm^2), and R_b is the bulk resistance (Ω) of a proton-conducting composite polymer membrane.

Typically, the R_b values of PVA/10 wt.%nt-TiO_2/PSSA composite membranes were on the order of 4–16 Ω and are highly dependent on the contents of PSSA polymer and nt-TiO_2 fillers, as shown in the inset of Fig. 5(a) for the high-frequency region. Note that these composite polymer membranes were immersed in D.I. water for 24 h before measurement.

Table 3 shows the ionic conductivities for PVA/0–10 wt.%nt-TiO_2/20 wt.%PSSA composite membranes at different temperatures in water. As seen in Table 3, the ionic conductivity value of

Table 3
Ionic conductivities (mS cm^{-1}) for PVA/*X* wt.%nt-TiO_2/20%PSSA composite polymer membranes in water at various temperatures.

Temp.	σ/S cm^{-1}			
	0 wt.%	3 wt.%	5 wt.%	10 wt.%
30 °C	4.58 ± 0.03	2.52 ± 0.02	1.54 ± 0.02	1.14 ± 0.01
40 °C	5.10 ± 0.02	2.75 ± 0.02	1.75 ± 0.03	1.24 ± 0.03
50 °C	5.68 ± 0.04	2.97 ± 0.04	1.88 ± 0.05	1.40 ± 0.04
60 °C	6.23 ± 0.05	3.25 ± 0.04	2.08 ± 0.04	1.55 ± 0.05
70 °C	7.00 ± 0.05	3.54 ± 0.05	2.33 ± 0.06	1.69 ± 0.06

PVA/20 wt.%PSSA composite membranes (without fillers) in water is 4.58×10^{-3} S cm^{-1} at 30 °C. Comparatively, the ionic conductivity values for PVA/*X* wt.%nt-TiO_2/20 wt.%PSSA composite membranes with 3, 5, and 10 wt.% nt-TiO_2 fillers are 2.52×10^{-3}, 1.54×10^{-3}, and 1.14×10^{-3} S cm^{-1} at 30 °C, respectively. It was found that the PVA/3 wt.%nt-TiO_2/20 wt.%PSSA composite membrane has the highest ionic conductivity, $\sigma = 2.52 \times 10^{-3}$ S cm^{-1}, at ambient temperature.

By contrast, Sahu et al. [24] showed an ionic conductivity of 1.30×10^{-3} S cm^{-1} for the PVA/PSSA polymer membrane in fully humidified condition at 30 °C. Moreover, they also showed that the ionic conductivity of a pristine PVA membrane was only 1.0×10^{-5} S cm^{-1} [24]. According to the above results, it is seen clearly that the ionic conductivity of the PVA/nt-TiO_2/20 wt.%PSSA composite membrane decreases when the content of added nt-TiO_2 fillers increases. As compared with the other literature data, Rhim et al. [20] also have reported for the cross-linked PVA polymer membranes using sulfosuccinic acid (SSA) (as a cross-linking agent) for the proton conductivity and the methanol permeability were in the range of 10^{-3} to 10^{-2} S cm^{-1} and 10^{-7} to 10^{-6} cm^2 s^{-1}, respectively, in the temperature range of 25–50 °C. Finally, Huang et al. [29] also studied the proton-conducting polymer membrane based on PVA and poly (vinyl pyrrolidone) (PVP) with SSA for the DMFC. They also showed the proton conductivity in the magnitude of 10^{-2} S cm^{-1} and the methanol permeability of 10^{-8} to 10^{-7} cm^2 s^{-1} for PVA/PVP/SSA composite membranes.

For our results, it was observed that the ionic conductivity of all PVA/nt-TiO_2/20 wt.%PSSA composite polymer electrolytes in water was on the order of 10^{-3} S cm^{-1} at ambient temperature. The temperature dependence of the ionic conductivity is of the Arrhenius type: $\sigma = \sigma_o \exp(-(E_a/RT))$, where σ_o is a pre-exponential factor, E_a is the activation energy, and T is the temperature in Kelvin. From the $\log_{10}(\sigma)$ vs. $1/T$ plots, as shown in Fig. 5(b), the activation energy (E_a) can be obtained for PVA/*X* wt.%TiO_2/20 wt.%PSSA composite polymer electrolytes, which is dependent on the content of nt-TiO_2 fillers. The E_a value of PVA/*X* wt.%TiO_2/20 wt.%PSSA composite membrane is approximately 12–15 kJ mol^{-1}, which is better than the general cross-linked composite polymer electrolyte membrane having E_a value over 20 kJ mol^{-1}. It is well known that the proton transport follows two mechanisms: the one is the Grotthus mechanism, which can be explained as the proton jump from one solvent molecule to the next through hydrogen bonds; the other is the vehicle mechanism, which assume that the proton diffuses together with solvent molecules by forming a complex (i.e., H_3O^+) and then diffuses intact. We assume that both the Grotthus and vehicle mechanisms may be responsible for the composite polymer membrane proton transfer. In addition, when the nt-TiO_2 filler used as a stiffener material is added into a PVA and PSSA host, the swelling ratio of composite polymer membranes was markedly reduced from 160 to 110% (detailed data not shown here). As expected, the thermal and mechanical properties, and dimensional stability were also improved.

All methanol permeabilities of PVA/nt-TiO_2/PSSA composite membranes were obtained from the slopes of the straight line for the methanol concentration vs. time curves. It is shown that the methanol permeabilities of the PVA/nt-TiO_2/20 wt.%PSSA composite membranes are 8.40×10^{-7} to 3.66×10^{-7} cm^2 s^{-1}. However, the permeability of the PVA/nt-TiO_2/PSSA composite membrane, measured to be on the order of 10^{-7} cm^2 s^{-1} in this study, is lower than that of Nafion 117 membrane, which is on the order of 2.91×10^{-6} cm^2 s^{-1} [25].

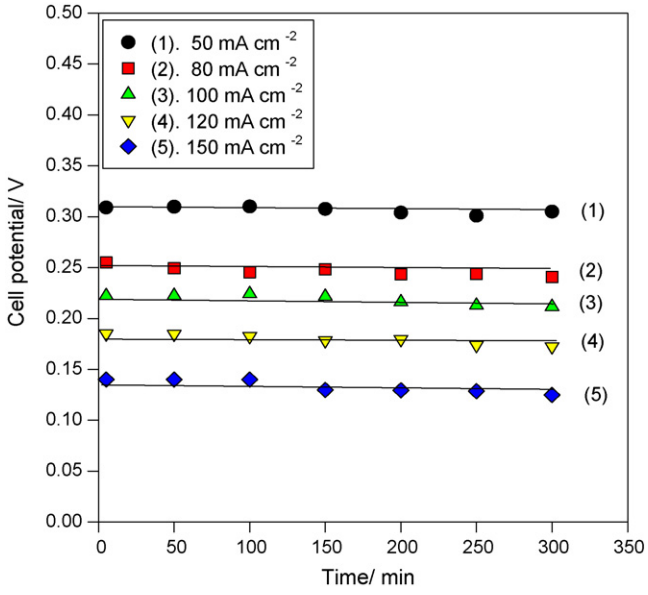

Fig. 6. The *E*–*t* curves for the DMFC using a PVA/5%nt-TiO_2/20 wt.%PSSA composite membrane with a 2 M methanol fuel at various current densities at 25 °C and in ambient air.

3.5. Electrochemical measurements

Fig. 6 shows the *E*–*t* curves of the DMFC consisting of the PtRu anode, the Pt/C cathode, using a PVA/5 wt.%TiO_2/20 wt.%PSSA composite membrane with a 2 M methanol fuel at various current densities, at 25 °C and in ambient air. The average cell potentials of the DMFC at the current densities of 50, 80, 100, 120, 150 mA cm^{-2} were 0.306, 0.246, 0.218, 0.179, and 0.133 V, respectively. In spite of a tendency of the cell potential to drop at the beginning of the test, the cell potentials were leveled and remained constant during the 10 h period. The performance of the DMFC using a PVA/5 wt.%nt-TiO_2/20 wt.%PSSA composite membrane with a 2 M methanol fuel was also examined at various constant cell potentials of 0.40, 0.30, 0.20, 0.15 V, respectively. It was found that the average current densities of the DMFC were 14.9, 51.6, 107.7, and 135.4 mA cm^{-2}, respectively. In spite of a tendency to fall at the beginning of the test, the current densities of the DMFC were almost invariant during the measurement; demonstrating good electrochemical properties.

Fig. 7 shows the potential–current density (*I*–*V*) and the power density–current density curves for an air-breathing DMFC with 1, 2, and 4 M methanol fuels at 25 °C, respectively. The highest peak power density of 23.72 mW cm^{-2} was achieved for the DMFC using a PVA/5 wt.%nt-TiO_2/20 wt.%PSSA composite membrane and a 2 M methanol fuel was achieved at $E_{p,max}$ = 0.160 V with a peak current density ($i_{p,max}$) of 148.1 mA cm^{-2}, as listed in Table 4. By comparison, the peak power density of a similar DMFC, only using a 1 M methanol fuel, was 12.85 mW cm^{-2} at $E_{p,max}$ = 0.151 V with a peak current density of 85.1 mA cm^{-2}. Measurements were made at 25 °C and 1 atm. Furthermore, the peak power density of the DMFC with a 4 M methanol fuel was only 10.99 mW cm^{-2} at $E_{p,max}$ = 0.10 V with a peak current density of 103.1 mA cm^{-2}.

Table 4
Electrochemical parameters for the DMFCs using the PVA/3 wt.%nt-TiO_2/20 wt.%PSSA composite polymer membrane with varied methanol concentrations at 25 °C and in ambient air.

Parameters	Conc.		
	1 M CH_3OH	2 M CH_3OH	4 M CH_3OH
E_{ocp}/V	0.50	0.60	0.44
Max. P.D./mW cm^{-2}	12.85	23.72	10.99
$i_{p,max}$/mA cm^{-2}	85.10	148.10	103.10
$E_{p,max}$/V	0.151	0.160	0.100

As a result, the peak power densities were in the order of 2 M methanol >1 M methanol >4 M methanol. Especially, the DMFC with a 2 M methanol fuel shows the highest power density (P.D. = 23.72 mW cm^{-2}) among these methanol concentrations, indicating an optimal range under these conditions. Importantly, our results compared with the literature data, in terms of the peak power density on the DMFC. Huang et al. [29] reported the peak power density of 5.20 mW cm^{-2} for their DMFC using a cross-linked PVA/PVP composite polymer membrane (a SIPN-20 sample) and a 2 M methanol/O_2 at room temperature; they also showed the peak power density of 5.26 mW cm^{-2} for Nafion 115 polymer membrane. More recently, Yang [30] studied a composite polymer membrane based on sulfonated poly(ether ether ketone) and sulfated poly(vinyl alcohol), i.e., SPEEK/PVA, for an acidic DMFC. They showed a peak power density value of around 21 mW cm^{-2} for the DMFC with a 2 M methanol/air at 80 °C.

Moreover, Lin et al. [31] prepared the proton-conducting hybrid membranes composed of PVA and phosphotungstic acid (PWA) for the DMFC. The electrochemical performance of PVA/PWA membrane and Nafion 115 exhibited almost equal peak power density of 5 mW cm^{-2}, at 20 mA cm^{-2} at ambient conditions. Lin et al. [32] also synthesized a semi-interpenetrating network (SIPN) membrane by using PVA with sulfosuccinic acid (SSA) as a cross-linking agent and poly(styrene sulfonic acid-*co*-maleic acid) (PSSA-MA) as a proton source for the DMFC. It was found that the peak power density of the DMFC with the SIPN membrane using 2 M methanol and oxygen gas was over 100 mW cm^{-2} at 80 °C. Yang [33] studied a composite membrane based on PVA and sulfated β-cyclodextrin for a DMFC. It was found that the peak power densities of the DMFCs with these

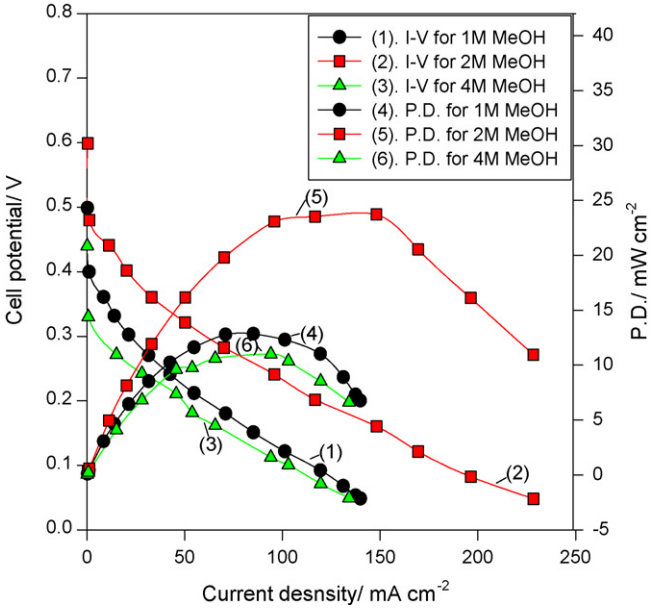

Fig. 7. The *I–V* and P.D. curves for the DMFC using PVA/5 wt.%nt-TIO_2/20 wt.%PSSA composite polymer membrane at 25 °C and in ambient air.

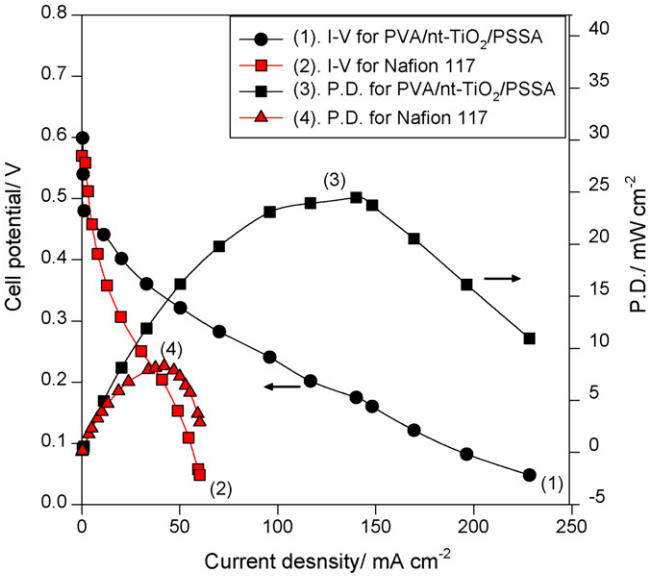

Fig. 8. Comparison of *I–V* and P.D. curves for the DMFC using a PVA/5 wt.%nt-TiO_2/20 wt.%PSSA and Nafion 117 proton membrane, both with a 2 M methanol fuel at 25 °C and in ambient air.

composite membranes were increased from 14.34 mW cm^{-2} up to 18.56 mW cm^{-2} at ambient conditions when the content of sulfated β-cyclodextrin increased from 10 to 23 wt.%.

Furthermore, Qiao et al. [34] prepared the proton-conducting composite membranes based on high molecular weight PVA and poly(2-acrylamido-2-methyl-1-propanesulfonic acid) (PAMPS) for DMFC applications. The peak power density of the DMFC fabricated with the acidic PVA/PAMPS membrane was 15.8 mW cm^{-2} at 30 °C, which reached 42.9 mW cm^{-2} at 80 °C. Recently, Bhat et al. [35] studied the poly(vinyl alcohol)/polystyrene sulfonic acid/mordenite (PVA/PSSA/MOR) composite blend membrane for DMFCs. The peak power density of 74 mW cm^{-2} was achieved for the DMFC using PVA/PSSA electrolyte with 50% degree of sulfonation and 10 wt.% mordenite (MOR) at 70 °C. These comparisons indicate that the DMFC comprised of the PVA/nt-TiO_2/PSSA composite membrane showed excellent electrochemical performance under ambient conditions.

It is well accepted that the proton-conducting polymer membrane with high open circuit potential corresponds to the low methanol crossover [23]. The reason for the poor electrochemical performance of the DMFC with 4 M methanol fuel may be in part due to the methanol crossover increase; it was because it showed the lowest open circuit potential (E_{ocp}) of 0.44 V, as shown in Table 4. By comparison, the open circuit potential of the DMFC with a 2 M methanol fuel reached about 0.60 V; it was the highest value among the three methanol concentrations. On the other hand, the other possible reason for the poor electrochemical performance may be due to the unstable MEA interface; it showed a higher activation resistance (R_{ct}) value. As seen in Fig. 8, it showed a large cell potential drop at a lower discharge current density region with a 4 M methanol fuel. It may conclude that the poor performance of the DMFC with a 4 M methanol fuel is due to both the methanol crossover increase and the unstable MEA interface.

The peak power density of the DMFC using the PVA/5 wt.%nt-TiO_2/20 wt.%PSSA composite membrane (peak P.D. = 23.72 mW cm^{-2}) was much better than that of the DMFC using Nafion 117 membrane (peak P.D. = 8.33 mW cm^{-2}), both a 2 M methanol fuel and at ambient conditions, as shown in Fig. 8. The merit is obvious that the novel PVA/nt-TiO_2/PSSA composite membrane is a cheap non-perfluorosulfonated polymer

membrane, as compared with Nafion 117 membrane; which is an expensive fully perfluorosulfonated polymer membrane.

4. Conclusions

The proton-conducting composite membranes based on the PVA, nt-TiO_2, and PSSA blends were prepared by a solution casting method. The ionic conductivities of the blend composite membranes are on the order of 10^{-3} S cm^{-1} in water at ambient temperature. It was found that the methanol permeability of the PVA/nt-TiO_2/PSSA composite membranes (on the order of 10^{-7} cm^2 s^{-1}) is lower than that of Nafion 117 membrane (on the order of 10^{-6} cm^2 s^{-1}). The air-breathing direct methanol fuel cell (DMFC) comprised of PVA/nt-TiO_2/PSSA composite polymer membrane was assembled and systematically examined. It was found that the highest peak power density of the DMFC was realized with a 2 M methanol fuel. Moreover, the peak power densities at ambient conditions are in the order of 2 M methanol >1 M methanol >4 M methanol.

The electrochemical performance, in terms of the peak power density, of the DMFC with the PVA/5 wt.%nt-TiO_2/20 wt.%PSSA composite membrane (peak P.D. = 23.72 mW cm^{-2}) is several times greater than that of the DMFC with Nafion 117 membrane (peak P.D. = 8.33 mW cm^{-2}), both with a 2 M methanol fuel and at ambient conditions. However, the electrochemical performance of the DMFC with a 4 M methanol fuel was poor, i.e., lower peak P.D. and open circuit potential, it is due to the higher methanol crossover rate and an unstable MEA interface. In summary, this PVA/nt-TiO_2/PSSA composite membrane is a viable candidate for DMFC applications.

Acknowledgements

Financial support from the National Science Council, Taiwan (Project No: NSC-96-2221-E131-009-MY2) is gratefully acknowledged.

References

[1] W.H. Lizcano-Valbuena, V.A. Paganin, E.R. Gonzalez, Electrochim. Acta 47 (2002) 3715–3722.
[2] N. Nakagawa, Y. Xiu, J. Power Sources 118 (2003) 248–255.
[3] G.G. Park, T.H. Yang, Y.G. Yoon, W.Y. Lee, C.S. Kim, Int. J. Hydrogen Energy 28 (2003) 645–650.
[4] H. Fukunaga, T. Ishida, N. Teranishi, C. Arai, K. Yamada, Electrochim. Acta 49 (2004) 2123–2129.
[5] V. Baglio, A.S. Arico, A.D. Blasi, V. Antonucci, P.L. Antonucci, S. Licoccia, E. Traversa, F.S. Fiory, Electrochim. Acta 50 (2005) 1241.
[6] T.C. Deivaraj, J.Y. Lee, J. Power Sources 142 (2005) 43–49.
[7] K. Furukawa, K. Okajima, M. Sudoh, J. Power Sources 139 (2005) 9–14.
[8] J.H. Choi, Y.M. Kim, J.S. Lee, K.Y. Cho, H.Y. Jung, J.K. Park, I.S. Park, Y.E. Sung, Solid State Ionics 176 (2005) 3031–3034.
[9] V.S. Silva, S. Weisshaar, R. Reissner, B. Ruffmann, S. Vetter, A. Mendes, L.M. Madeira, S. Nunes, J. Power Sources 145 (2005) 485–494.
[10] B.E. Hayden, D.V. Malevich, D. Pletcher, Electrochem. Commun. 3 (2001) 395–399.
[11] E. Antolin, Mater. Chem. Phys. 78 (2003) 563–573.
[12] G.Q. Lu, C.Y. Wang, J. Power Sources 144 (2005) 141–145.
[13] C.Y. Yang, P. Yang, J. Power Sources 123 (2003) 37–42.
[14] T. Shimizu, T. Momma, M. Mohamedi, T. Osaka, S. Sarangapani, J. Power Sources 137 (2004) 277–283.
[15] K. Kordesch, V. Hacker, U. Bachhiesl, J. Power Sources 96 (2001) 200–203.
[16] J.G. Liu, T.S. Zhao, R. Chen, C.W. Wong, Electrochem. Commun. 7 (2005) 288–294.
[17] B.K. Kho, I.H. OH, S.A. Hong, H.Y. Ha, Electrochim. Acta 50 (2004) 781–785.
[18] C.C. Yang, Y.J. Lee, J.M. Yang, J. Power Sources 188 (2009) 30–37.
[19] C.C. Yang, Y.J. Lee, Thin Solid Films 517 (2009) 4735–4740.
[20] J.W. Rhim, H.B. Park, C.S. Lee, J.H. Jun, D.S. Kim, Y.M. Lee, J. Membr. Sci. 238 (2004) 143–151.
[21] T. Yang, Q. Xu, Y. Wang, B. Lu, P. Zhang, Int. J. Hydrogen Energy 33 (2008) 1014–1022.
[22] T. Yang, Int. J. Hydrogen Energy 33 (2008) 6772–6779.
[23] G.G. Kumar, P. Uthirakumar, K.S. Nahm, R.N. Elizabeth, Solid State Ionics 180 (2009) 282–287.
[24] A.K. Sahu, G. Selvarani, S.D. Bhat, S. Pitchumani, P. Sridhar, A.K. Shukla, N. Narayanan, A. Banerjee, N. Chandrakumar, J. Membr. Sci. 319 (2008) 298–305.
[25] S. Panero, P. Fiorenza, M.A. Navarra, J. Romanowska, B. Scrosati, J. Electrochem. Soc. 152 (12) (2005) A2400–A2405.
[26] H.Y. Chang, C.W. Lin, J. Membr. Sci. 218 (2003) 295–306.
[27] C.C. Yang, C.T. Lin, S.J. Chiu, Desalination 233 (2008) 137–146.
[28] T. Kasuga, Thin Solid Films 496 (2006) 141–145.
[29] Y.F. Huang, L.C. Chuang, A.M. Kannan, C.W. Lin, J. Power Sources 186 (2009) 22–28.
[30] T. Yang, J. Membr. Sci. 342 (2009) 221–226.
[31] C.W. Lin, R. Thangamuthu, C.J. Yang, J. Power Sources 253 (2005) 23–31.
[32] C.W. Lin, Y.F. Huang, A.M. Kannan, J. Power Sources 171 (2007) 340–347.
[33] T. Yang, Int. J. Hydrogen Energy 34 (2009) 6917–6924.
[34] J. Qiao, T. Okada, H. Ono, Solid State Ionics 180 (2009) 1318–1323.
[35] S.D. Bhat, A.K. Sahu, C. George, S. Pitchumani, P. Sridhar, N. Chandrakumar, K.K. Singh, N. Krishna, A.K. Shukla, J. Membr. Sci. 340 (2009) 73–83.